Full characterization of PDX, a neuroprotectin/protectin D1 isomer, which inhibits blood platelet aggregation.

Ping Chen, Bernard Fenet, Sabine Michaud, Nick Tomczyk, Evelyne Véricel, Michel Lagarde, Michel Guichardant

Full characterization of PDX, a neuroprotectin/protectin D1 isomer, which inhibits blood platelet aggregation.

Chen P.[a], Fenet B.[b], Michaud S[a]., Tomczyk N.[c], Véricel E.[a], Lagarde, M[a]. and Guichardant M[a*].

[a] Université de Lyon; Inserm UMR 870; Insa-Lyon, RMND/IMBL; Inra 1235; 69621 Villeurbanne, France.
[b] CCRMN-UCB-Lyon 1-ESCPE
[c] Waters Corporation – Atlas Park, Simonsway, Manchester, M22 5PP, UK.

[*] Corresponding author. Tel.:+ 33 4 72 43 82 15; Fax:+ 33 4 72 43 85 24
E-mail address: michel.guichardant@insa-lyon.fr

Key-words:
Docosahexaenoic acid
15-lipoxygenase
10,17-dihydroxy-docosahexaenoic acid
Double lipoxygenation
Ion mobility separation

Abbreviations: BSTFA, *N,O*-Bis(trimethylsilyl)-trifluroroacetamide; HFBI, heptafluorobutyryl imidazole; DHA, docosahexaenoic acid; sLOX , soybean lipoxygenase

ABSTRACT

Our study aimed to establish the complete structure of the main dihydroxy conjugated triene issued from the lipoxygenation (soybean enzyme) of docosahexaenoic acid (DHA), named PDX, an isomer of protectin/neuroprotectin D1 (PD1/NPD1) described by Bazan & Serhan. NMR approaches and other chemical characterization (e.g. GC-MS, HPLC and LC-MS/MS) indicated that PDX is 10(S),17(S)-dihydroxy-docosahexa-4*Z*,7*Z*,11*E*,13*Z*,15*E*,19*Z*-enoic acid. The use of $^{18}O_2$ and mass spectrometry showed that PDX is a double lipoxygenation product. Its structure differs from PD1, with *E,Z,E* geometry (PDX) instead of *E,E,Z* (PD1) and S configuration at carbon 10 instead of R. PDX inhibits human blood platelet aggregation at sub-micromolar concentrations.

1. Introduction

Docosahexaenoic acid (DHA) oxygenated metabolism has been investigated and increasing interest arose recently for dihydroxy-docosahexaenoic acid (DHA) derivatives, especially neuroprotectin D1 (NPD1) described in brain tissues by Bazan et al. [1,2]. Its structure has been established by Serhan et al. as 10(R),17(S)-dihydroxy-docosahexa-4*Z*,7*Z*,11*E*,13*E*,15*Z*,19*Z*-enoic acid [3-5] in T helper type 2-skewed peripheral blood mononuclear cells as a 15/n-6 lipoxygenase-dependent product, and termed protectin D1 (PD1).

In mammalian cells NPD1/PD1 results from the 15-lipoxygenation of docosahexaenoic acid (DHA) *via* an epoxidation mechanism [1] as already reported for leukotriene B_4 formation [6]. Resolvin D1 and PD1, as well as mono-hydroxy-DHA products, were found to be produced by human whole blood and neutrophils [7], trout head-kidney [8], and stroke-injuried murine brain tissues [9]. In contrast, the PD1 isomer, 10,17(S)-dihydroxy-docosahexa-4*Z*,7*Z*,11*E*,13*Z*,15*E*,19*Z*-enoic acid, reported by Butovich [10-11] could result from a double lipoxygenation mechanism, although this was not evidenced. Furthermore, the latter report did not state the configuration of carbon 10 and did not claim any biological function. The goal of the present study was to characterize the configuration of carbon 10 and geometry of the conjugated triene in PD1 isomer, called PDX, issued from either the n-6 lipoxygenation of either DHA, or 10(±)-hydroxy-docosahexa-4*Z*,7*Z*,11*E*,13*Z*,16*Z*,19*Z*-enoic acid, or 17(S)-hydroxy-docosahexa-4*Z*,7*Z*,10*Z*,13*Z*,15*E*,19*Z*-enoic acid. Characterization used homodecoupling NMR techniques and UPLC-MS/MS with the Waters SYNAPT HDMS system and the integrated ion mobility separation. Stereochemistry of carbon 10 was assessed by HPLC and GC-MS approaches, and the mechanism of lipoxygenation was determined by using $^{18}O_2$. It is concluded that PDX is 10(S),17(S)-dihydroxy-docosahexa-4*Z*,7*Z*,11*E*,13*Z*,15*E*,19*Z*-enoic acid produced by double lipoxygenation of DHA.

Preliminary data regarding the inhibitory effect of PDX on platelet aggregation are also given.

2. Materials and methods

2.1. Reagents

Docosahexaenoic acid (DHA, C22:6), leukotriene B_4, soybean lipoxygenase (sLOX, EC 1.13.11.12, Type 1-B, 131,000 units/mg solid) were purchased from Sigma-Aldrich, 10(±)-hydroxy-docosahexa-4*Z*,7*Z*,11*E*,13*Z*,16*Z*,19*Z*-enoic acid (10(±)-HDoHE), and 8(R)- and 8(S)-HETEs were from Cayman Chemical Co. For the materials used in GC-MS analyses, platinum oxide (PtO_2) and *N*,*O*-Bis(trimethylsilyl)-trifluroroacetamide (BSTFA) were products of Sigma-Aldrich, heptafluorobutyryl imidazole (HFBI) was from Interchim. Pestipur organic solvents were from Carlo-Erba. All chemicals used were reagent grade or with the highest quality available.

2.2. Chiral HPLC separation of 10(±)-HDoHE

Stereoisomers from methylesters of 10(±)-HDoHE were isolated by isocratic chiral HPLC on a 4.6 × 250 mm Chiralcel OD-H column hold at 25°C. The mobile phase was n-hexane/2-propanol (100:2, v/v) pumped at a flow rate of 1 mL/min. 10(R)-HDoHE and 10(S)-HDoHE were detected at 235 nm and collected. Methylesters of 8(R)- and 8(S)-HETEs were used as corresponding homologs of 10(R)- and 10(S)-HDoHE, respectively.

2.3. Biosynthesis of 17(S)-hydroxy (HDoHE) and 10,17-dihydroxy (diHDoHE) DHA derivatives, as well as 8,15-diHETEs from 8(R)- and 8(S)-HETE

Reactions were catalyzed by soybean lipoxygenase (sLOX type 1-B) in sodium-borate buffer under normal or $^{18}O_2$ atmosphere (PDX production from DHA). DHA was treated by

sLOX, hydroperoxides were reduced by $NaBH_4$, the incubate was acidified to pH 3, and di- and mono-hydroxylated fatty acids were extracted using a C_{18} solid-phase cartridge with 10 mL of ethanol. They were further dried under a stream of nitrogen.

Similarly, 2 µM of either 17(S)-HDoHE (produced from DHA) or 10(R)-HDoHE, or 10(S)-HDoHE isolated by chiral HPLC as described above, were treated by sLOX to generate 10,17-diHDoHE. 8,15-diHETEs were obtained by the same way from commercial sources of 8(R)- or 8(S)-HETE.

2.4. Purification of monohydroxylated and dihydroxylated fatty acids

Mono- and dihydroxylated fatty acids were analyzed by reverse phase high performance liquid chromatography (RP-HPLC) on a Waters XBridge C18 column (4.6 x 250 mm, 3.5 µm) using a linear solvent gradient (1 mL/min): A was a mixture of acetonitrile/water acidified to pH 3 (10:90, v/v), and B was acetonitrile. Conjugated diene monohydroxylated and conjugated triene dihydroxylated fatty acids were detected using a diode array detector at 235 nm and 270 nm, respectively, and collected separately.

2.5. GC-MS analysis of diHDoHE

DiHDoHE isolated by HPLC were hydrogenated using platinum oxide, and derivatized into methyl esters and trimethylsilyl ethers. Samples were then analyzed by GC-MS using electron impact mode (EI) to localize the hydroxyl groups in the fatty chain.

2.6. Nuclear magnetic resonance (NMR) of PDX

NMR spectra were acquired on a BRUKER drx500 spectrometer equipped with a 5 mm TXI probe. Experiments were driven at 25°C on 2 mg of samples dissolved in 450 µL of CD_3OD.

2.7. UPLC-MS of 10,17-diHDoHE and ion mobility

Dihydroxylated-DHA isomers were analyzed on the Waters® SYNAPT™ HDMS™ system in MS mode coupled directly to the Acquity® UPLC® with a BEH™ -C_{18} 1.7 µm, 1.0 mm x 100 mm column. The separation was performed at 40°C at a flow rate of 0.25 mL/min using a mobile phase system which consisted of acetonitrile/water (containing 0.1% of formic acid) that was run as a linear gradient to reach 100% acetonitrile (containing 0.1% of formic acid) after 6 min. MS data were acquired from 50 to 1000 m/z at 10 spectra/sec rate.

The ion mobility of PDX and Isomer 1 (obtained from the lipoxygenation of 10(S)-HDoHE) were measured on the SYNAPT HDMS system in HDMS mode. All samples were infused at a flow rate of 10 µL/min and ionized using electrospray ionization-mass spectrometry (ESI). ESI-MS/MS was performed on the M+Na adduct and mobility separations were performed with nitrogen admitted to ion mobility cell at a pressure of 0.5 mbar. Data extraction and analysis were performed with MassLynx™ and Driftscope™ software.

3. **Results and Discussion**

3.1. Metabolites of DHA obtained after soybean 15-lipoxygenase (sLOX)treatment

DHA was a good substrate for sLOX and led to a main compound eluted at 51.6 min (Fig. 1A). This compound was identified as 17(S)-HDoHE since it had the same retention time as commercially available 17(R)-HDoHE on reverse phase HPLC, but separated from it by chiral HPLC, both compounds having the same UV spectrum with λ_{max} = 235 nm. In addition, a main product called PDX, eluted at 35.4 min, and was detected at 270 nm (Fig. 1B), as well as five minor compounds, all with a conjugated triene structure according to their UV spectra (see below). The minor conjugated trienes had shorter retention times compared

to PDX, but their amounts were much too low (the whole five compounds represented less than 5% of the amount of PDX) to allow their characterization.

The UV spectrum of PDX (Fig. 1b inset) showed a maximum absorption at λ = 270 nm with two smooth shoulder peaks at λ = 260 nm and λ = 280 nm indicating the presence of a conjugated triene. Moreover, the left shoulder peak was higher than the right shoulder one suggesting that the triene geometry could likely be *E,Z,E*, as observed with 8(S),15(S)-di-HETE and 5(S),12(S)-diHETE which have the same triene geometry (results not shown). UV spectra of these compounds differ from compounds with a *Z,E,E* configuration such as leukotriene B_4 (LTB_4) and 12-epi-LTB_4, for which both right and left sharp shoulder peaks have nearly the same height (results not shown). In our conditions, the yield conversion rate of DHA by sLOX was estimated at 10% for the monohydroxy derivative and 3% for the dihydroxy one (PDX).

3.2. *Localization by GC-MS of hydroxy groups on the chain*

For this purpose, PDX was derivatized as described in "Materials & Methods".

GC-MS spectrum of the hydrogenated PDX derivative showed characteritic ions at m/z: 515 (M-15, loss of CH_3), 459 (M-71 loss of CH_2^+-$(CH_2)_3$-CH_3), 369 (M-(71+90)), 359 (M-171, loss of CH_2-$(CH_2)_7$-$COOCH_3$), 273 (base peak, Me_3SiO^+-CH_2-$(CH_2)_7$-$COOCH_3$), 173 (Me_3SiO^+-CH_2-$(CH_2)_4$-CH_3) and 73 ($SiMe_3$) (Fig. 2A). PDX synthesized under $^{18}O_2$ atmosphere revealed a shift of the fragments ion mass of 2 or 4 (Fig. 2B), indicating the insertion of ^{18}O at both carbons 10 and 17 (m/z at 519 and 463 instead of 515 and 459, and 371, 275, 175 and 131 instead of 369, 273, 173 and 129).

3.3. *Determination of carbon 10 stereochemistry*

If the stereochemistry of carbon 17 is S according to the well known properties of sLOX [12], that of carbon 10 remained to be determined. For this purpose, 17(S)-HDoHE prepared from DHA treated by sLOX, and 10(S)- and 10(R)-HDoHE separated by chiral chromatography from 10(±)-HDoHE, were incubated separately with sLOX followed by hydroperoxide reduction. Two diastereo-isomers were eluted by HPLC (Fig. 3B) at 36.7 and 37.1 min. The first peak was attributed to 10(S),17(S)-diHDoHE and the second to 10(S),17(R)-diHDoHE, according to the separation (Fig. 3A) of 8(S),15(S)- and 8(R),15(S)-diHETEs synthesized from 8(S)-HETE and 8(R)-HETE, respectively [13]. Moreover, the former diHETE also co-eluted with commercial 8(S),15(S)-diHETE. In addition, the lipoxygenation of 17(S)-HDoHE led to a dihydroxy derivative that co-eluted with 10(S),17(S)-diHDoHE (not shown).

Finally, PDX synthesized from DHA, co-eluted with 10(S),17(S)-diHDoHE issued from 10(S)-HDoHE (Fig. 3C) whereas 10(R),17(S)-diHDoHE from 10(R)-HDoHE was eluted 0.5 min later, as shown in Fig. 3B, which indicates that PDX has the S stereochemistry at carbon 10, and the same *E,Z,E* geometry of the conjugated triene, as already described for AA dioxygenation [14].

The complete structure was also confirmed by using a new UPLC-MS/MS system including an ion mobility interface which is able to discriminate between different isotopologues which differ in their structure. For this purpose, 10(S),17(S)-diHDoHE and PDX were analyzed by UPLC using electrospray ionization as described in “Materials & Methods”. The mass spectrum of PDX (Fig. 4A) was superimposable to that of 10(S),17(S)-diHDoHE, with the same main ion at m/z 383 corresponding to the sodium adduct. In addition, the HDMS infusion data of PDX and 10(S),17(S)-diHDoHE, where the M+Na was isolated in

the quadrupole, showed that they have identical drift time which indicates they have the same collisional cross sectional areas. This is shown by the mobilograms of PDX and 10(S),17(S)-diHDoHE (Fig. 4B) which are fully superimposable except for a small contaminant detected in 10(S),17(S)-diHDoHE. This is again in agreement with PDX being 10(S),17(S)-dihydroxy-docosahexa-4*Z*,7*Z*,11*E*,13*Z*,15*E*,19*Z*-enoic acid.

Overall, these results are in favour of a double lipoxygenation with a S,S configuration as expected according to similar mechanism which has already been reported for some diHETEs from arachidonic acid. This is valid for 5(S),12(S)-dihydroxy-eicosatetraenoic acid (5(S),12(S)-diHETE), which results from the oxygenation of 12(S)-hydroxy-eicosatetraenoic acid (12(S)-HETE) by 5-lipoxygenase, or 5(S)-HETE by 12-lipoxygenase [15-17], and for 5(S),15(S)-diHETE through 5- and 15-lipoxygenases [18]. This hypothesis was validated by using $^{18}O_2$ since both hydroxyl groups at carbon 10 and 17 were labelled. According to these results, which complete and fit with previous data from Butovich, we can definitely conclude that 15-soybean lipoxygenase produces PDX *via* a double lipoxygenation of DHA. PDX differs from the initially described 10,17(S)-docosatriene by Hong et al. (7), further named PD1.

3.4. Determination by different NMR techniques of the PDX conjugated triene geometry

Taking into account that the stereochemistry of carbon 10 has not yet been assigned, it was important to verify the geometry of double bounds, provided that PD1 has an R configuration at carbon 10, with a *E,E,Z* triene as reported by Serhan et al. [3]. Sequential attribution of protons and carbon atoms *via* a high resolution HSQC-TOCSY experiment (starting from each edge of the molecule), and high resolution 2D matrix (Fig. 5) allow a good sequential identification of spin systems. 11-12-13 and 14-15-16 spin systems at the center of the molecule were quite indistinguishable (same proton and same carbon chemical shifts),

which in fact confirms the symmetrical structure of the triene segment. We used a modified HSQC-TOCSY experiment (IPAP hsqc-gpsp) [19] to increase resolution for AB spin systems, and a 30 ms mixing time to get more information from those very near cross peaks. At this stage, the attribution of all protons and carbons confirms the results of previous works of Butovich [10]. However, collected NMR data presented in Table 1 showed that the acidic carbon is missing in the ^{13}C spectrum, and remains not determined.

In a second step, we measured proton J coupling constants in the conjugated triene. The easiest part was $J_{11,12}$ and $J_{15,16}$, because of the AX character of spin system. A simple 1D proton spectrum with multisite homodecoupling [20] of H13-H14 and H10-H17 led to $J_{11,12}$ $=J_{15,16}$=15Hz (Fig. 6A) demonstrating the E character of these two double bonds. At the end, the measurement of $J_{13,14}$ was more difficult to get because of second order effects between H_{13} and H_{14}, and superimposition of carbon signals. However, we succeeded to get a good measurement by the SAPHIR method [21] (Fig. 6B). The heart of the method was based on the asymmetry introduced in the AB system by the diluted carbon 13 isotope. Considering a 2D HSQC experiment acquired without ^{13}C decoupling, the response of the couple H_{13}-$^{13}C_{13}$ was split in a doublet with J_{CH} = 158Hz, whereas the H_{14}-$^{12}C_{14}$ neighbor was at the center of this doublet, cancelling second order effects. In addition, the homodecoupling of all other coupled protons during acquisition led to simple couple of proton doublets separated by J_{CH}. The measurement of $J_{H13-H14}$=11Hz gave the evidence that this double bond was in a Z geometry.

As a confirmation, in a last step, we simulated (Fig. 6C) the spectrum of the central part of the molecule with the BRUKER DAISY spin simulator. 10 spins were taken into account, and the result was very close to the acquired spectrum, confirming the determination. This NMR study confirms that the geometry of the conjugated triene in PDX is 11*E*,13*Z*,15*E*.

3.5. Inhibition of platelet aggregation by PDX

PDX incubated with platelet suspension at different concentrations ranged from 0.3 µM to 10 µM inhibited collagen-induced platelet aggregation in a dose-dependent manner (Fig. 7). 25% and 75% inhibition were observed at 0.3 µM and 1 µM of PDX, respectively.

4. **Conclusions**

We conclude from the present data that the main dihydroxylated compound issued from the 15-lipoxygenation of DHA by the soybean enzyme is PDX. Its structure, 10(S),17(S)-dihydroxy-docosahexa-4*Z*,7*Z*,11*E*,13*Z*,15*E*,19*Z*-enoic acid, differs from PD1 described as 10(R),17(S)-dihydroxy-docosahexa-4*Z*,7*Z*,11*E*,13*E*,15*Z*,19*Z*-enoic acid [3]. Moreover, PDX exhibits interesting inhibition of human blood platelet aggregation.

Acknowledgments

This study was supported by INSERM and the French Ministry of Education and Research. Ping Chen was a recipient of a PhD Student grant from China.

References

[1] Mukherjee, P.K., Marcheselli, V.L., Serhan, C.N. and Bazan, N.G. (2004) Neuroprotectin D1: a docosahexaenoic acid-derived docosatriene protects human retinal pigment epithelial cells from oxidative stress. Proc. Natl. Acad. Sci. U S A. 101, 8491-8496.

[2] Bazan, N.G. (2005) Neuroprotectin D1 (NPD1): a DHA-derived mediator that protects brain and retina against cell injury-induced oxidative stress. Brain Pathol. 15, 159-166.

[3] Serhan, C.N., Gotlinger, K.H., Hong, S., Lu, Y., Siegelman, J., Baer, T., Yang, R., Colgan, S.P. and Petasis, N.A. (2006) Anti-inflammatory actions of neuroprotectin

D1/protectin D1 and its natural stereoisomers: assignments of dihydroxy-containing docosatrienes. J. Immunol. 176, 1848-1859. Erratum in: J. Immunol. 176, 3843.

[4] Ariel, A., Li, P-L., Wang, W., Tang, W-X., Fredman, G., Hong, S., Gotlinger, K.H. and Serhan, C.N. (2005) The docosatriene Protectin D1 is produced by TH_2 skewing and promotes human T cell apoptosis via lipid raft clustering. J. Biol. Chem. 280, 43079-43086.

[5] Bazan, N.G., Marcheselli, V.L. and Cole-Edwards, K. (2005) Brain response to injury and neurodegeneration: endogenous neuroprotective signaling. Ann. N Y Acad Sci. 1053, 137-147.

[6] Panossian, A., Hamberg, M. and Samuelsson, B. (1982) On the mechanism of biosynthesis of leukotrienes and related compounds. FEBS Lett. 150, 511-513.

[7] Hong, S.K., Gronert, K., Devchand, P.R., Moussignac, R-L. and Serhan, C.N. (2003) Novel docosatrienes and 17S-Resolvins generated from docosahexaenoic acid in murine brain, human blood, and glial cells, J. Biol. Chem. 278, 14677-14687.

[8] Hong, S.K., Tjonahen, E., Morgan, E. L., Lu, Y., Serhan, C.N. and Rowley, A.F. (2005) Rainbow trout (Oncorhynchus mykiss) brain cells biosynthesize novel docosahexaenoic acid-derived resolvins and protectins-Mediator lipidomic analysis, Prostaglandins other Lipid Mediat. 78, 107-116.

[9] Marcheselli, L.V., Hong, S., Lukiw, W.J., Tian, X.H., Gronert, K., Musto, A., Hardy, M., Gimenez, J.M., Chiang, N., Serhan, C.N. and Bazan, N.G. (2003) Novel docosanoids inhibit brain ischemia reperfusion mediated leukocyte infiltration and proinflammatory gene expression, J. Biol. Chem. 278, 43807-43817.

[10] Butovich, I.A. (2005) On the structure and synthesis of neuroprotectin D1, a novel anti-inflammatory compound of the docosahexaenoic acid family, J. Lipid Res. 46, 2311-2314.

[11] Butovich, I.A. (2006) A one-step method of 10,17-dihydro(pero)xydocosahexa-4Z,7Z,11E,13Z,15E,19Z-enoic acid synthesis by soybean lipoxygenase, J. Lipid Res. 47, 854-863.

[12] N.G. Bazan, Neurotrophins induce neuroprotective signaling in the retinal pigment epithelial cell by activating the synthesis of the anti-inflammatory and anti-apoptotic neuroprotectin D1, Adv Exp Med Biol. 613 (2008) 39-44.

[13] Maas, R.L., Brash, A.R, Oates, J.A. (1981) A second pathway of leukotriene biosynthesis in porcine leukocytes, Proc. Nat. Acad. Sci. USA 78, 5523-5527.

[14] Van Os, C.P., Rijke-Schilder, G.P., Van Halbeek, H., Verhagen, J. and Vliegenthart, J.F. (1981) Double dioxygenation of arachidonic acid by soybean lipoxygenase-1. Kinetics and regio-stereo specificities of the reaction steps, Biochim Biophys Acta. 663, 177-193.

[15] Lindgren, J.A., Hansson, G. and Samuelsson, B. (1981) Formation of novel hydroxylated eicosatetraenoic acids in preparations of human polymorphonuclear leukocytes, FEBS Lett. 128, 329-335.

[16] Marcus, A.J., Broekman, M.J., Safier, L.B., Ullman, H.L., Islam, N., Serhan, C.N., Rutherford, L.E., Korchak, H.M. and Weisssmann, G. (1982) Formation of leukotrienes and other hydroxyl acids during platelet-neutrophil interactions in vitro, Biochem. Biophys. Res. Commun. 109, 130-137.

[17] Borgeat, P.B., Fructeau de Laclos, B., Picard, S., Drapeau, J., Vallerand, P. and Corey, E.J. (1982) Studies on the mechanism of formation of the 5S,12S-dihydroxy-6,8,10,14(E,Z,E,Z)-icosatetraenoic acid in leukocytes, Prostaglandins 23, 713-724.

[18] Maas, R.L., Turk, J., Oates, J.A. and Brash, A.R. (1982) Formation of a novel dihydroxy acid from arachidonic acid by lipoxygenase-catalyzed double oxygenation in rat mononuclear cells and human leukocytes, J. Biol. Chem. 257, 7056-7067.

[19] Ronald, C., Crouch, C., Spitzer, T. D. and Martin, G.E. (1992) Strategies of the phase editing of relayed responses in 2D HMQC-TOCSY spectra Mag. Res. Chem. 30, 71-73.

[20] Hammarstroem, A., Otting, G. (1994) Improved Spectral Resolution in 1H NMR Spectroscopy by Homonuclear Semiselective Shaped Pulse Decoupling during Acquisition, J. Am. Chem.Soc. 116, 8847-8848.

[21] Vatele J.M., Fenet, B. and Eynard, T. (1998) Complete 13C assignments and structural elucidation of n-3 polyunsaturated fatty acids by the use of a new 2D NMR technique: SAPHIR-HSQC, Chem. Phys. Lipids. 94, 239-250.

Figure legends:

Fig. 1. Typical RP-HPLC profile of DHA derivatives. DHA was incubated with sLOX and lipid extract was analyzed by reverse phase HPLC: (a) Monohydroxylated fatty acids (λ = 235 nm); (b) dihydroxylated fatty acids (λ =270 nm).

Fig. 2. Mass-spectrum of the Me-TMS derivative of the hydrogenated PDX synthesized from DHA by sLOX under normal (A) or $^{18}O_2$ (B) atmosphere.

Fig. 3. Typical RP-HPLC profile of dihydroxylated fatty acids issued from 8(S)- and 8(R)-diHETE, and from 17-HDoHE stereoisomers (R and S): (A) The upper tracing shows 8(S),15(S)-diHETE and 8(R),15(S)-diHETE synthesized from 8(S)- and 8(R)-diHETE treated by sLOX; (B) Typical RP-HPLC profile of 10(S),17(S)-diHDoHE and 10(R),17(S)-diHDoHE synthesized from 10(±)-HDoHE; (C) Typical RP-HPLC profile of 10(S),17(S)-diHDoHE and 10(R),17(S)-diHDoHE plus PDX synthesized from DHA.

Fig. 4. Analysis of PDX by UPLC-MS/MS using an ion mobility interface: (A) full LC-MS/MS spectra of Isomer 1 and PDX; (B) Mass extracted mobilograms of Isomer 1 and PDX from full scan MS/MS.

Fig. 5. Sequential attribution of PDX with IPAP hsqc-tocsy. The figure is the overlay of two matrices: the sum of in-phase IP hsqc-tocsy and anti-phase AP hsqc-tocsy experiment, and the difference of the two matrices. Empty regions are cut to increase the resolution drawing. Ns=16, time domain td2=2048 td1=2048, processing domain si2=2048, si1=2048 with linear prediction.

Fig. 6. NMR techniques applied to PDX to achieve the double bond configuration: (A) Zooming of H11 and H16 signals: bottom: normal proton spectrum; top: with simultaneously homodecoupling of H13-H14 and H10-H17. The simultaneous two sites decoupling driven by frequency modulation of homodecoupling signal (standard Bruker sequence zghc) were the shape pulse used in the decoupling sequence, tuned to irradiate the wanted frequencies. (B) SAPHIR-HSQC method for measuring J coupling constant in the AB spin system H13-14. HSQC without carbon decoupling was used during acquisition and simultaneous homodecoupling of H12-H15 and H11-H16. The measured coupling constant was $J_{13,14}$=11Hz; (C) Comparison between the simulated spectrum (upper window) and the experimental spectrum (lower window). The spectrum of the central part of the molecule containing the triene motif with the two hydroxyl groups was simulated with the BRUKER DAISY spin simulator (upper window) and compared to the acquired spectrum (lower window). Non informative region was hidden with the cutting tool of MestReNova processing software.

Fig. 7. Dose-dependent inhibition of platelet aggregation by PDX. Human isolated blood platelet suspensions were incubated with different concentrations of PDX (0.3 to 10 µM). Aggregation was triggered by collagen and monitored for 4 min.

Table 1: ^{1}H and ^{13}C measured chemical shifts and proton coupling constants of PDX in CD3OD at 25°C. For AB spin systems, the values were refined by spectral simulation.

	proton		Carbon
Atom number	**δ, ppm**	**Coupling constant Hz**	**ppm**
1			**N.D.**
2	**2.347**	m	**34.298**
3	**2.39**	m	**23.022**
4	**5.406**	m	**128.300**
5	**5.409**	m	**129.047**
6	**2.822**	t, J(6,5)=J(6,7)=5.35	**25.704**
7	**5.467**	m	**130.009**
8	**5.461**	m	**125.516**
9	**2.4**	m, J(9,10)=6.5	**35.350**
10	**4.198**	J(10,11)=6.3, J(10,12)=1.3	**72.043**
11	**5.757**	J(11,12)=15	**137.127**
12	**6.747**	J(12,13)=11, J(12,14)=-0.8	**125.476**
13	**5.991**	J(13,14)=11, J(13,15)=-0.8	**128.966**
14	**5.995**	J(14,15)=11	**128.985**
15	**6.741**	J(15,16)=15, J(15,17) =1.3	**125.476**
16	**5.744**	J(16,17)=6.3	**137.066**
17	**4.174**	J(17,18)=6.5	**72.142**
18	**2.320**	m	**35.210**
19	**5.387**	m	**124.446**
20	**5.493**	m	**133.674**
21	**1.2**	J(21,22)=7.05	**20.667**
22	**0.983**	7.5	**13.518**

Figure 1

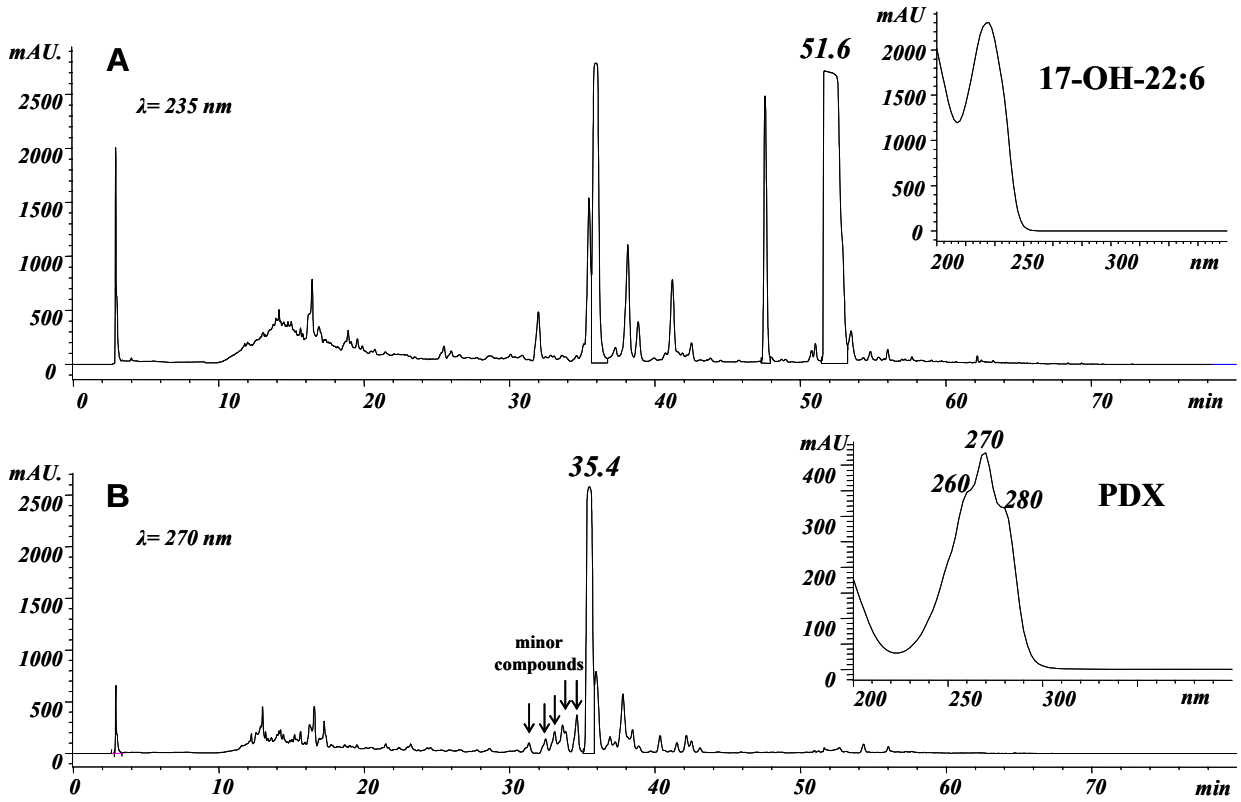
A
λ= 235 nm
mAU.
51.6
17-OH-22:6
mAU
nm
min
B
λ= 270 nm
35.4
minor
compounds
270
260
280
PDX

Figure 2

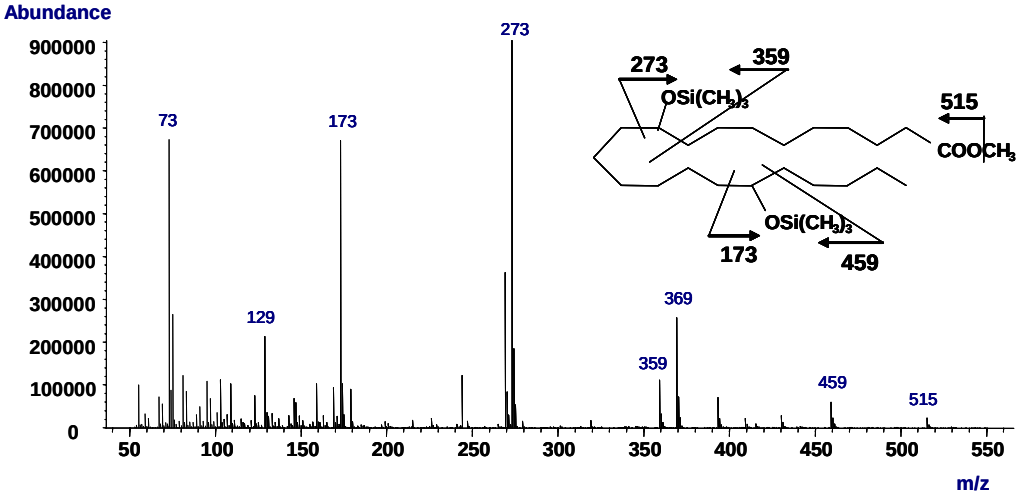
Abundance
900000
800000
700000
600000
500000
400000
300000
200000
100000
0
50
100
150
200
250
300
350
400
450
500
550
m/z
73
129
173
273
359
369
459
515
273
359
OSi(CH3)3
515
COOCH3
OSi(CH3)3
173
459

A

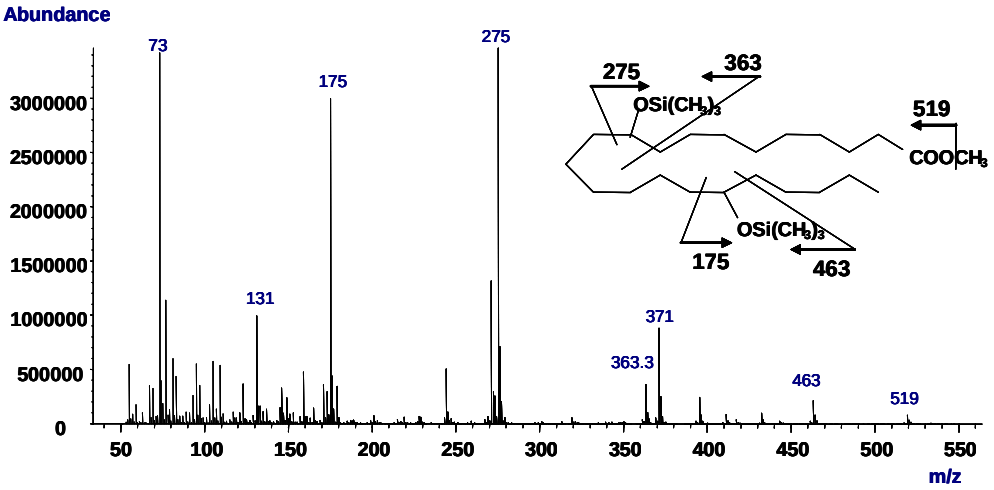
Abundance
3000000
2500000
2000000
1500000
1000000
500000
0
50
100
150
200
250
300
350
400
450
500
550
m/z
73
131
175
275
363.3
371
463
519
275
363
OSi(CH3)3
519
COOCH3
OSi(CH3)3
175
463

B

Figure 3:

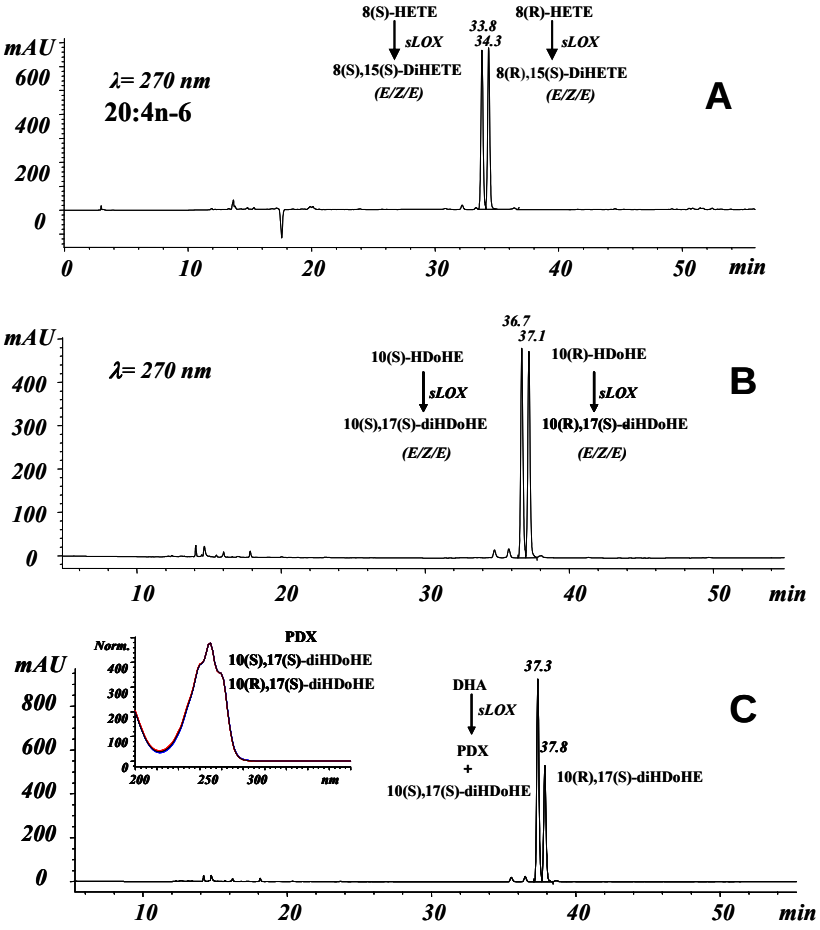
mAU
600
400
200
0
λ= 270 nm
20:4n-6
8(S)-HETE
sLOX
8(S),15(S)-DiHETE
(E/Z/E)
33.8
34.3
8(R)-HETE
sLOX
8(R),15(S)-DiHETE
(E/Z/E)
A
0
10
20
30
40
50
min
mAU
400
300
200
100
0
λ= 270 nm
36.7
37.1
10(S)-HDoHE
sLOX
10(S),17(S)-diHDoHE
(E/Z/E)
10(R)-HDoHE
sLOX
10(R),17(S)-diHDoHE
(E/Z/E)
B
10
20
30
40
50
min
mAU
800
600
400
200
0
Norm.
400
300
200
100
0
200
250
300
nm
PDX
10(S),17(S)-diHDoHE
10(R),17(S)-diHDoHE
DHA
sLOX
PDX
+
10(S),17(S)-diHDoHE
37.3
37.8
10(R),17(S)-diHDoHE
C
10
20
30
40
50
min

A

B

Figure 4:

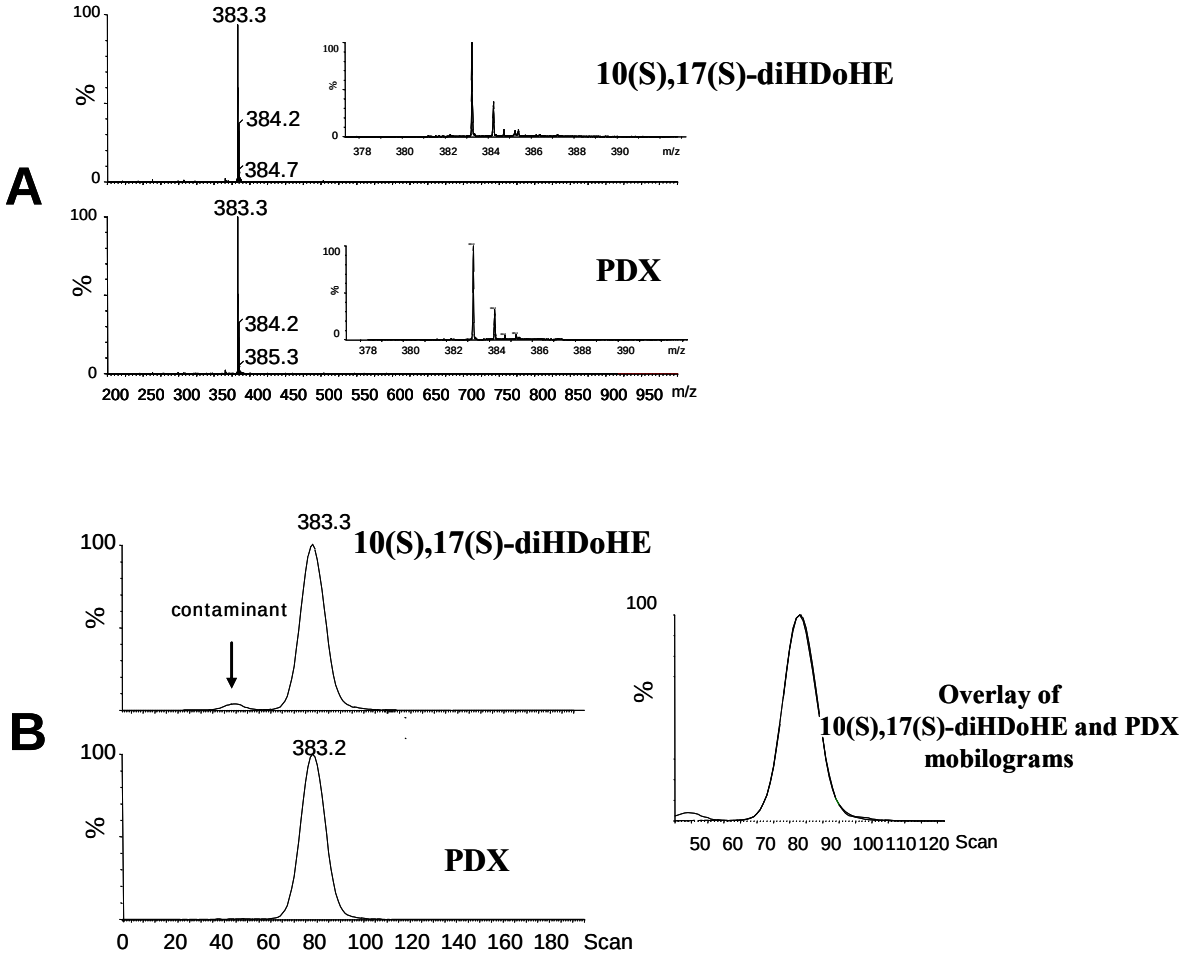
A
10(S),17(S)-diHDoHE
383.3
384.2
384.7
PDX
383.3
384.2
385.3
200 250 300 350 400 450 500 550 600 650 700 750 800 850 900 950 m/z
B
10(S),17(S)-diHDoHE
383.3
contaminant
PDX
383.2
0 20 40 60 80 100 120 140 160 180 Scan
Overlay of
10(S),17(S)-diHDoHE and PDX
mobilograms
50 60 70 80 90 100 110 120 Scan

Figure 5:

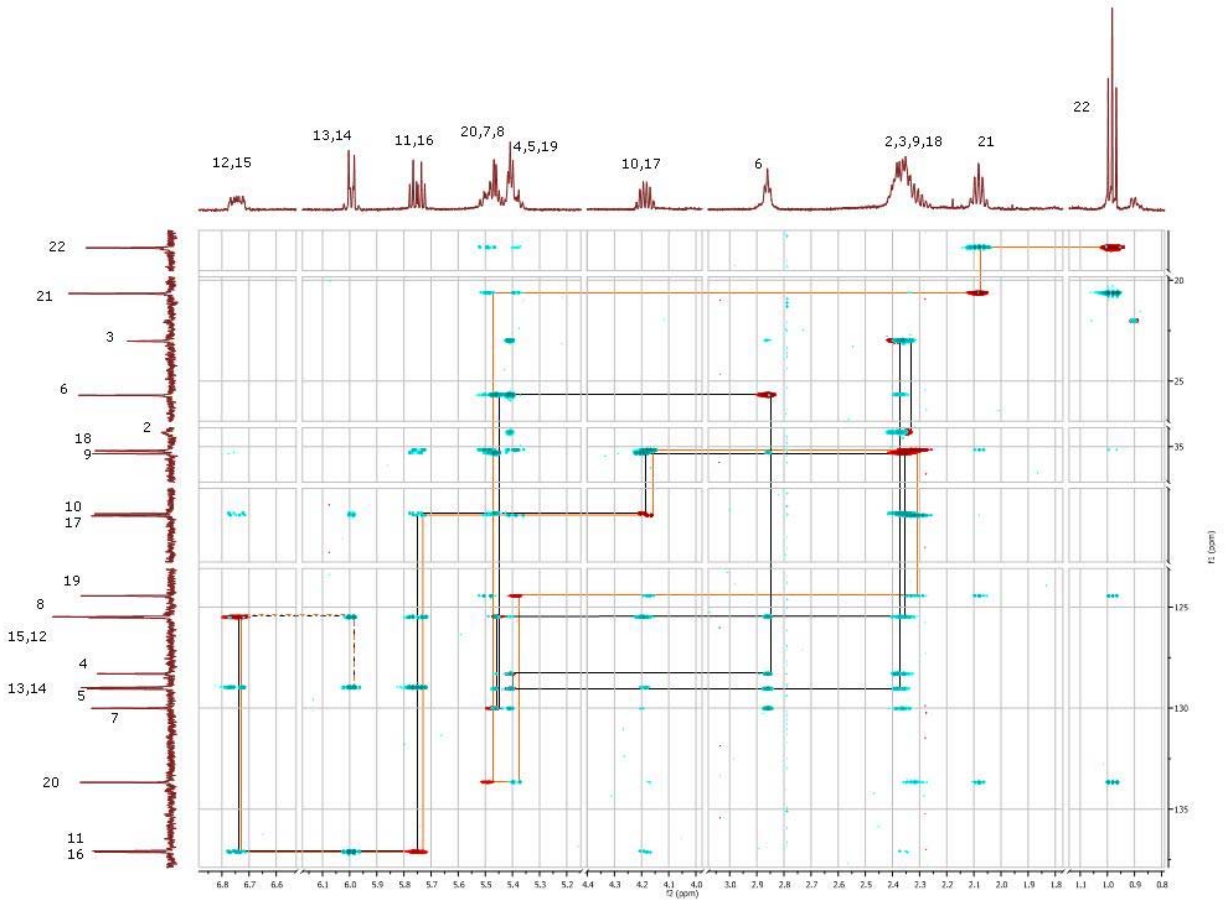
12,15
13,14
11,16
20,7,8
4,5,19
10,17
6
2,3,9,18
21
22
22
21
3
6
2
18
9
10
17
19
8
15,12
4
13,14
5
7
20
11
16

Figure 7:

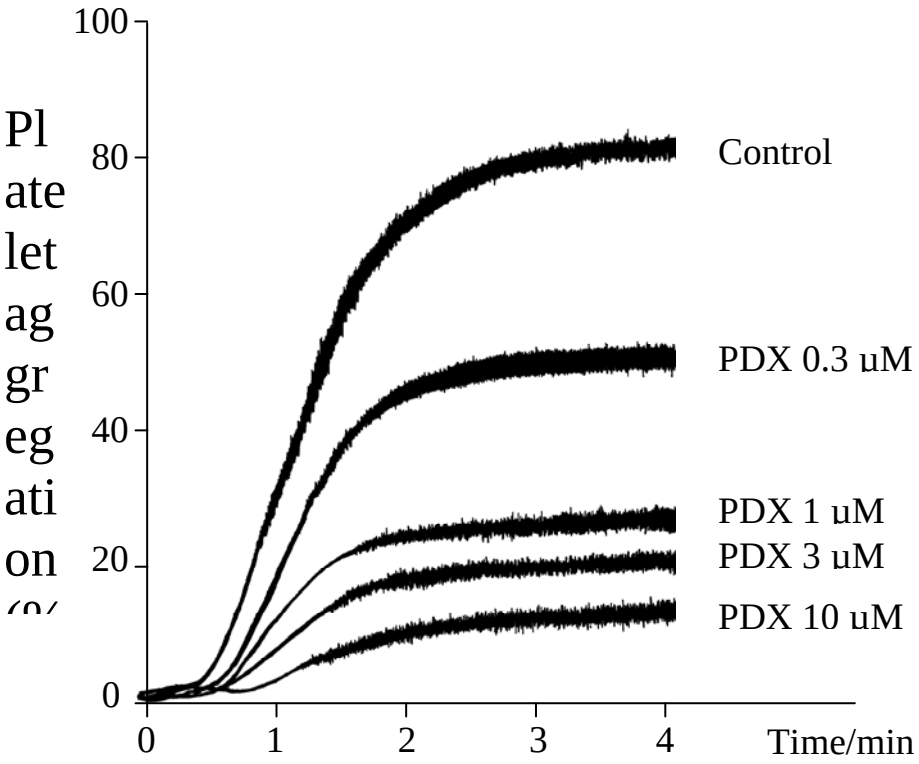
Platelet aggregation (%
100
80
60
40
20
0
0
1
2
3
4
Time/min
Control
PDX 0.3 uM
PDX 1 uM
PDX 3 uM
PDX 10 uM